Design of Luminescent Inorganic Materials: New Photophysical Processes Studied by Optical Spectroscopy

DANIEL R. GAMELIN AND HANS U. GÜDEL

Department of Chemistry and Biochemistry, University of Bern, Freiestrasse 3, CH-3000 Bern 9, Switzerland

Received July 12, 1999

ABSTRACT

Recent spectroscopic results in the emerging area of transition-metal NIR-to-visible upconversion are related. The examples of Ti^{2+}-, Re^{4+}-, and Os^{4+}-doped materials showing upconversion illustrate GSA/ESA, GSA/ETU, and photon avalanche multiphoton excitation mechanisms, respectively. Strategies for manipulation of such upconversion processes using the spectroscopic or magnetic properties of the host material are described. High-resolution low-temperature continuous-wave absorption and emission and time-resolved emission experiments combine to yield information about energy splittings, intensities, and excited-state dynamics, and assist in the design and development of luminescent materials showing novel multiphoton excitation properties.

I. Introduction

Advances in the development of new luminescent inorganic materials have traditionally involved contributions from both academic and industrial research groups. Fundamental research in this area has ultimately led to the application of luminescent inorganic materials in a wide variety of commercial settings, including such commonly encountered items as color televisions and fluorescent lighting tubes, as well as more specialized applications such as fiber amplifiers, plasma display screens, and quantum counters.[1] The combination of emission with other chemical, optical, magnetic, and conducting properties of inorganic materials is also an area showing immense promise and rapid progress, and is at the heart of several nascent molecular technologies.[2] The functions of many promising new materials often involve energy and/or electron transfer. A thorough understanding of these mechanisms is clearly invaluable for the rational

design and optimization of such materials. Because of the nature of the luminescence phenomenon itself, the search for new phenomena or applications involves an interplay between design synthesis and spectroscopic characterization, and includes interdisciplinary collaboration between chemists, physicists, and engineers.

In this Account, we relate some recent results involving the use of spectroscopy in the emerging area of transition-metal (TM) upconversion and describe two strategies for manipulation of these processes using the spectroscopic or magnetic properties of the host material. The host materials in this research are well-known crystalline materials having low phonon energies, and into these the TM is doped. The upconversion phenomena are closely associated with the electronic structures of the dopant ions, however, and are not limited to these hosts. This research has been spawned by our parallel efforts in several related areas of TM and rare-earth (RE) spectroscopy and electronic structure. Three areas of research in our laboratories that will not be described in this Account, but which are of equal relevance to the general topic of luminescent inorganic materials, are (a) the spectroscopic characterization of RE upconversion in low-phonon host matrixes,[3] (b) the development and characterization of new broadband emitters and potential laser materials involving d^1 and d^2 TMs,[4] and (c) detailed description of excited-state electronic structure in d^6 TM complexes with polypyridyl or related ligation.[5] All of these rely on high-resolution absorption and luminescence spectroscopy of single crystals at cryogenic temperatures, using polarized light where applicable. In special cases, we have also used the technique of luminescence line narrowing, or the application of external pressures or magnetic fields. Studies using pulsed excitation allow dynamic processes such as energy transfer to be probed. Combined, these techniques provide significantly more information about energy splittings, intensities, and excited-state dynamics than low-resolution spectra of solutions or glasses at room temperature. This information is highly valuable in the characterization of excited states and may assist the development of more advanced photonics materials.

II. Upconversion

Upconversion (UC),[6,7] simultaneous two-photon absorption (STPA),[8] and second-harmonic generation (SHG)[9] (Figure 1) are well-established methods for generation of short-wavelength radiation from long-wavelength pump sources. In contrast with SHG, which generates new frequencies through the (relatively) weakly wavelength-dependent hyperpolarizability of a substance, and STPA, which requires only one real excited state, upconversion relies on sequential discrete absorption and luminescence steps for shorter-wavelength generation, and hence on the presence of multiple metastable excited states. Whereas SHG requires coherent radiation, upconversion does not. Upconversion has been demonstrated as an efficient process for producing highly excited species that show

Daniel R. Gamelin received his B.A. from Reed College and his Ph.D. from Stanford University. His Ph.D. research, supervised by Edward Solomon, was in bioinorganic spectroscopy. He held a Swiss NSF postdoctoral fellowship at the University of Bern, and has recently joined the chemistry faculty at the University of Washington, Seattle.

Hans U. Güdel was born and educated in Switzerland. He received his Ph.D. in 1969 from the University of Bern, working with Andreas Ludi. He worked as a postdoc with Carl Ballhausen (Copenhagen) and James Ferguson (Canberra) for a total of four years before joining the chemistry faculty at the University of Bern. He became a professor in 1978, spent time as a visiting professor at the University of Copenhagen in 1982, a visiting scholar at Stanford University in 1983–84, and a visiting scientist at the Los Alamos National Laboratory and the Hughes Research Laboratories in 1992–93. His primary research interests are in the optical and magnetic properties of new transition-metal and rare-earth-metal compounds.
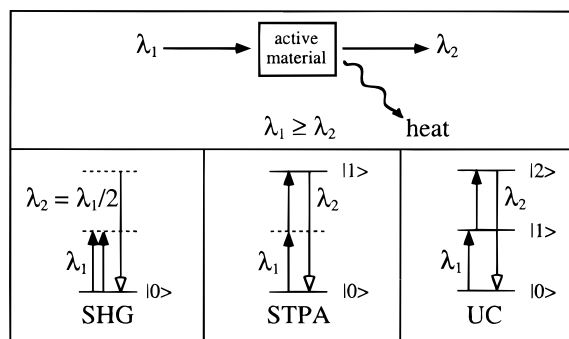
FIGURE 1. Schematic illustration of second-harmonic generation (SHG), simultaneous two-photon absorption (STPA), and upconversion (UC) processes capable of converting low-energy photon input into higher-energy photon output. The horizontal dashed (solid) lines indicate virtual (discrete) levels.

spontaneous or stimulated emission at wavelengths significantly shorter than those of excitation.

The minimum prerequisite for generation of upconversion luminescence by a material is the existence of two metastable excited states, the first serving as an excitation reservoir, and the second as the emitting state. RE ions are particularly well suited to satisfy this prerequisite. Due to the shielding of their f electrons, RE ions are characterized by an extreme insensitivity to their environment. As a result, RE excited states typically luminesce if separated from the nearest lower excited state by at least ca. 5 quanta of the highest frequency nuclear vibration.[10] RE ions often have a series of luminescent f−f excited states, in contrast with Kasha's rule for organic chromophores,[11] which states that typically only the lowest state of a given spin multiplicity will luminesce. Since the first observations of upconversion in the mid-1960s, hundreds of studies on RE upconversion involving most of the lanthanide and actinide ions have been reported.[6] In many cases, efficient three- or four-quantum upconversion is observed. Recent milestones include the development of all-solid-state RE upconversion lasers operable at room temperature[7] and the demonstration of a viable three-dimensional imaging technique based on RE upconversion.[12]

Our contributions in RE upconversion have mainly centered on the use of host lattices with low phonon energies, i.e., chlorides and bromides.[3] With respect to the commonly studied oxides and fluorides, multiphonon relaxation is significantly less efficient in the heavier halides, leading to new excited-state dynamics and emission properties. Recently, we have been interested in expanding the repertoire of available upconversion sensitizer and activator ions in the search for new luminescent materials and photophysical processes. We have synthesized and explored the photophysical properties of a variety of TM-doped halide hosts, in some cases in combination with lanthanide doping. The use of TMs in this way is appealing in view of their rich coordination chemistry, redox behavior, and magnetic properties, which provide opportunities to couple their chemical properties with the photophysical properties of interest, as has been done in many other areas of inorganic luminescence. The same properties that make TMs accessible to chemical and

magnetic perturbation, namely the poorer shielding of the d orbitals, also lead to greater intrinsic luminescence quenching mechanisms, however, and the ability of upconversion to compete with nonradiative relaxation is generally more tenuous. In this Account, we present results from three TM upconversion systems studied in our laboratories, chosen to illustrate three important mechanisms for generating upconversion luminescence.

III. Transition-Metal Upconversion Case Studies

A. Excited-State Absorption (ESA) in Ti^{2+}:$MgCl_2$. The first TM upconversion observed in our laboratories was found in Ti^{2+} doped into $MgCl_2$.[13] As shown in the d^2 energy-level diagram of Figure 2a, octahedral Ti^{2+} has an orbitally degenerate $^3T_1(t_2^2)$ ground state. This is split in $MgCl_2$ due to a weak trigonal (D_{3d}) distortion, yielding a $^3A_2$ ground state.[13] The 10 K axial absorption spectrum of 5% Ti^{2+}: $MgCl_2$ is shown in Figure 3a. Two features are observed in the visible and near-IR (NIR) energy regions, corresponding to the first two spin-allowed electronic transitions from the ground state ($^3T_1(t_2^2) \rightarrow {}^3T_2(t_2e)$ and $^3T_1 \rightarrow {}^3T_1(t_2e)$). From Figure 2, a number of spin-forbidden ($^3T_1 \rightarrow {}^1\Gamma$) electronic transitions are also expected in this same energy region, but these carry extremely small oscillator strengths due to the spin selection rule $\Delta S = 0$, and are unobservable in absorption. The lowest-energy of these is the $^1E(D_{3d})$ component of the $^1T_1(t_2^2)$ octahedral parent state. This excited state is located at 7665 cm^{-1} using emission spectroscopy (Figure 3b). As a result of the inverse relationship between oscillator strength and radiative decay rate, this NIR luminescence has an extremely long lifetime of 109 ms at 10 K. A second luminescence is observed from the $^3T_1(t_2e)(O_h)$ higher excited state (13 340 cm^{-1} maximum) at low temperatures ($T < 100$ K). This upper-excited-state luminescence is only possible due to the large energy gap below the $^3T_1(t_2e)(O_h)$ emitting state (Figure 2) and is assisted by the low vibrational energies of the chloride host material. Detailed spectroscopic studies have been used to quantify the radiative and nonradiative decay processes involving these two excited states in Ti^{2+}:$MgCl_2$.[13]

The upper-excited-state ($^3T_1$) luminescence is observed not only with higher-energy excitation, but also with broadband excitation in the NIR using a lamp.[13] At low excitation powers, this upconversion luminescence shows a quadratic dependence on excitation power, as would be expected from a two-photon process. Shown in Figure 3c is the excited-state excitation (ESE) spectrum of this sample, obtained by pumping the $^3T_2(t_2e)$ absorption at 9300 cm^{-1} and monitoring the visible upconversion luminescence intensity as a function of the wavelength of a second NIR beam. This ESE spectrum shows features not observed in the ground-state absorption (GSA) spectrum. They reflect ESA transitions from the long-lived $^1E(D_{3d})$ level and are assigned as the $^1E(D_{3d}) \rightarrow {}^1A_1(t_2^2)$ and $^1T_2(t_2e)(O_h)$ transitions, respectively, on the basis of their energies and band shapes. The $^1E(D_{3d}) \rightarrow {}^3T_1(t_2e)(O_h)$ ESA transition, which should occur in the same energy region,
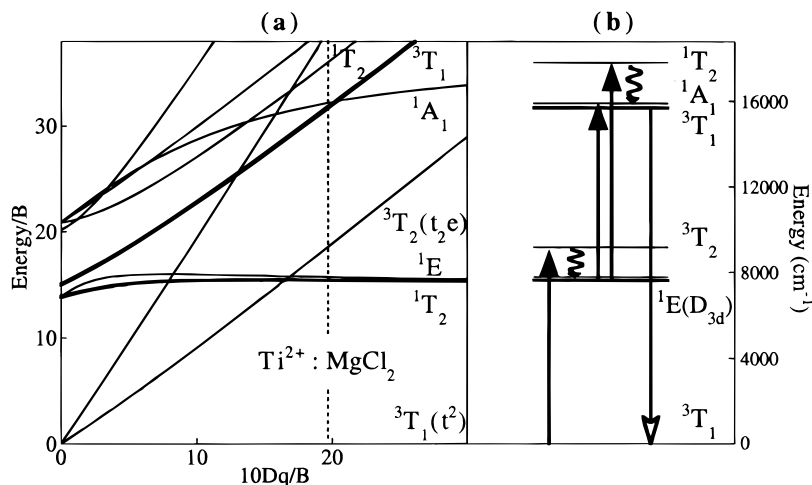
FIGURE 2. (a) Energy levels of a d^2 ion in an octahedral environment as a function of ligand-field strength 10 Dq and the Racah parameter B. The vertical dashed line indicates the position of Ti^{2+}:$MgCl_2$ in this diagram. The bold lines indicate the luminescent excited states of Ti^{2+}. (b) GSA/ESA upconversion mechanism in Ti^{2+}:$MgCl_2$. Only the spin-allowed transitions are observed. Curly arrows represent rapid multiphonon relaxation.
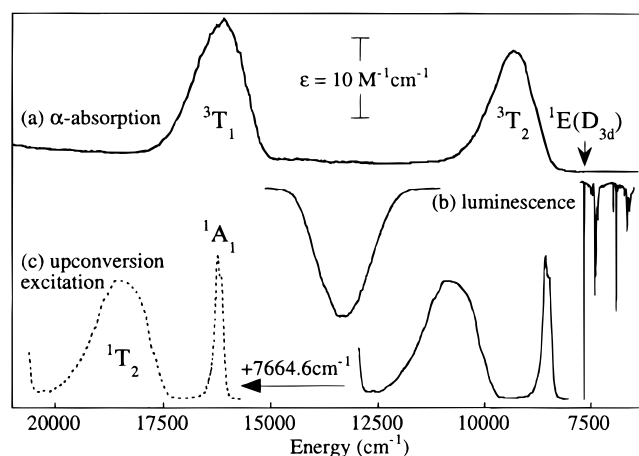

FIGURE 3. 10 K spectra of 5% Ti^{2+}:$MgCl_2$. (a) Axial (α) absorption, (b) luminescence, and (c) two-color upconversion excitation, the first color exciting the $^3T_2$ absorption at 9300 cm^{-1}. The dashed line in (c) is the same as the full line but has been shifted to higher energy by 7664.6 cm^{-1}, the energy of the metastable $^1E(D_{3d})$ origin, and thus shows the true energies of the $^1A_1$ and $^1T_2$ excited states. Adapted from ref 13.

is not observed due to the stringent adherence to spin selection rules in this ion. GSA therefore provides a probe of the triplet excited states, while the $^1E(D_{3d})$ ESE spectrum provides a probe of the singlet excited states. The mechanism for generation of visible luminescence from NIR excitation thus involves sequential GSA and ESA steps, as described by Figure 2b. The first photon promotes the ion to the long-lived intermediate $^1E(D_{3d})$ excited state via $^3T_1(t_2{}^2) \rightarrow {}^3T_2(t_2e)$ GSA followed by fast multiphonon relaxation, and a second photon then promotes the ion to the upper excited state by $^1E(D_{3d}) \rightarrow {}^1A_1(t_2{}^2)$ or $^1T_2(t_2e)$ ESA, followed by rapid multiphonon relaxation to the luminescent $^3T_1$ state. This single-ion mechanism is the simplest process by which higher excited states may be produced, and is one of the most important and efficient upconversion mechanisms operative in RE upconversion materials.

Table 1. Transition Metals for Which Upconversion Luminescence Has Been Demonstrated, Including Relevant Mechanistic and Electronic-Structural Information[a]

ion	electrons	representative host	UC mechanism	ζ (crystal, cm^{-1})
Ti^{2+}	$3d^2$	$MgCl_2$	two-color GSA/ESA	100
Ni^{2+}	$3d^8$	$CsCdCl_3$	GSA/ESA, avalanche	620
Mo^{3+}	$4d^3$	Cs_2NaYCl_6	two-color GSA/ESA	600
Re^{4+}	$5d^3$	Cs_2ZrCl_6	ETU	2300
Os^{4+}	$5d^4$	Cs_2ZrBr_6	GSA/ETU, GSA/ESA, avalanche	2600
Pr^{3+}	$4f^2$	$LaCl_3$		749
Tm^{3+}	$4f^{12}$	$LaCl_3$		2638

[a] The lightest and heaviest lanthanides showing single-ion upconversion are also listed.

Ti^{2+}:$MgCl_2$ provides a clear example of the role of spin selection rules in 3d TM photodynamics. Such selection rules are more dramatic in the 3d TMs than in RE ions due to the smaller spin−orbit coupling parameter, ζ, in the former (Table 1). In Table 1, ζ values of the lightest (Pr^{3+}) and heaviest (Tm^{3+}) lanthanides capable of mediating single-ion upconversion are shown for comparison. Large spin−orbit coupling convolutes the spin and orbital contributions to the multielectron wave functions involved in an electronic transition, making spin a poor quantum descriptor, and thus relaxing spin selection rules. As shown in Table 1, ζ in Ti^{2+} is roughly an order of magnitude smaller than in those commonly studied RE upconversion ions.

B. Energy-Transfer Upconversion in Re^{4+}:Cs_2ZrCl_6. More recently, a number of studies have been undertaken in our laboratories with the specific aim of designing TM systems that display upconversion luminescence.[14−17] We have initially focused on the d^3 and d^4 electronic configurations, since such ions have multiple ligand-field-independent excited states, and some are known in the literature to luminesce from upper excited states.[18] Octahedral Re^{4+} has a $(5d)^3$ electron configuration with an
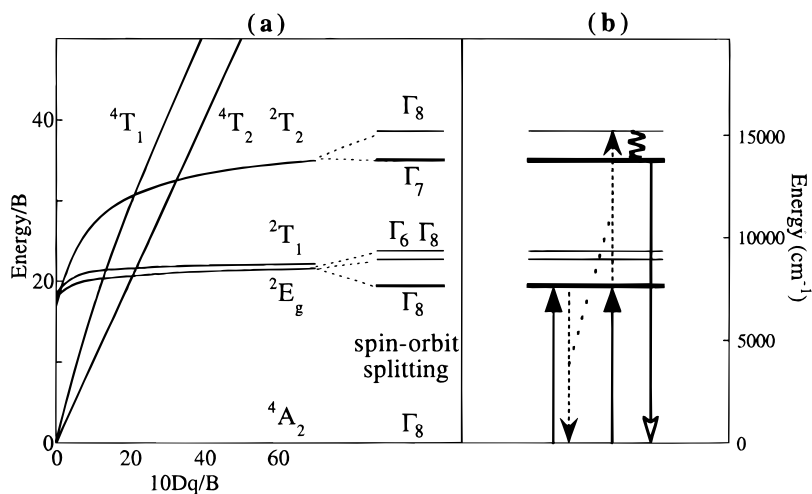
FIGURE 4. (a) Energy-level diagram for a d^3 ion in an octahedral environment, and the energy levels of $Re^{4+}:Cs_2ZrCl_6$ after spin–orbit splitting. The luminescent states of Re^{4+} are indicated by bold lines. (b) GSA/ETU mechanism observed in $Re^{4+}:Cs_2ZrCl_6$. Dashed arrows indicate the nonradiative energy-transfer upconversion step. The curly arrow represents rapid multiphonon relaxation.

orbitally nondegenerate $^4A_2$ ground state and two sets of ligand-field-independent doublet excited states to higher energy, as shown in Figure 4. These excited states are substantially split due to the large spin–orbit coupling in this 5d element (Table 1). Figure 5a,b shows the 10 K absorption and luminescence properties of 2.5% $Re^{4+}:Cs_2$-$ZrCl_6$. Luminescence from both the $\Gamma_8(^2T_1)$ (7695 cm^{-1}) and $\Gamma_7(^2T_2)$ (13 885 cm^{-1}) excited states is observed. These luminescent states are separated from the nearest lower excited states by energy gaps of 12 and 22 quanta, respectively, of the highest frequency nuclear vibration, $\nu_1(a_1)$ = 342 cm^{-1}. The $\Gamma_8(^2T_1)$ excited state has a 10 K lifetime of 1.98 ms, which decreases to 0.91 ms at 300 K, while the $\Gamma_7(^2T_2)$ excited state has a 10 K lifetime of 0.12 ms that decreases to 0.05 ms at 300 K. Variable-temperature absorption and luminescence studies show that both lifetimes are purely radiative even at 300 K,[17] and the $\Gamma_7(^2T_2)$ lifetime is shorter than that of $\Gamma_8(^2T_1)$ primarily because of the additional interexcited-state luminescence channels available to this upper excited state.

Excitation into the $^2T_1/^2E$ absorption features in the range between 7500 and 9500 cm^{-1} results in intense visible luminescence from the higher-energy $\Gamma_7(^2T_2)$ excited state.[15] At low powers a purely quadratic power dependence is observed, but at higher powers this dependence becomes linear.[17] The one-color upconversion excitation spectrum at 10 K is shown in Figure 5c and follows very closely the absorption spectrum (Figure 5a) at this and all other temperatures. The excitation spectrum lacks new features that could be associated with ESA transitions, as observed in $Ti^{2+}:MgCl_2$, but rather indicates that the specific energy of excitation is not important as long as the system is excited by GSA into the $^2T_1/^2E$ manifold. This strongly implicates an energy-transfer upconversion (ETU) mechanism. In contrast with the GSA/ESA mechanism of $Ti^{2+}:MgCl_2$, GSA/ETU is a multi-ion process. Two ions excited to the intermediate level by GSA participate in a nonradiative transfer of one ion's
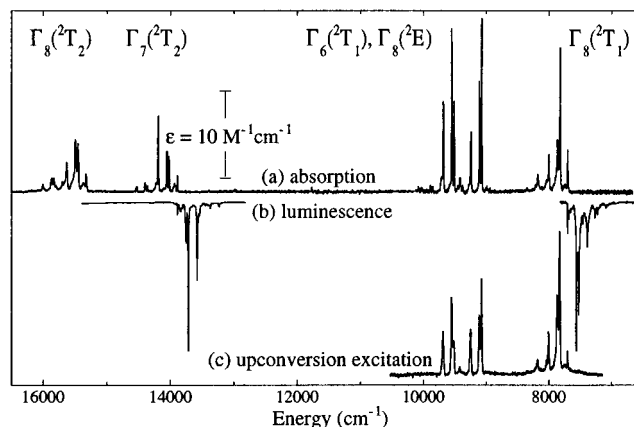

FIGURE 5. 10 K spectra of 2.5% $Re^{4+}:Cs_2ZrCl_6$. (a) Absorption, (b) luminescence, and (c) upconversion excitation. Adapted from refs 15 and 17.

excitation energy to the other, resulting in one ion in the ground state and one ion in the upper excited state. This is illustrated in Figure 4b for $Re^{4+}:Cs_2ZrCl_6$.

The ETU mechanism is confirmed by time dependence measurements, in which the visible upconversion luminescence intensity is probed following a 10-ns NIR excitation pulse. These data are shown in Figure 6c, in comparison with the decay curves observed upon low-power direct excitation into the intermediate (Figure 6b) and upper (Figure 6a) levels. From these data, two significant observations can be made: (i) the upconversion luminescence shows a distinctly slow rise time following the excitation pulse, and (ii) it decays substantially more slowly following NIR excitation than it does following direct excitation. These observations are readily explained as follows. The laser pulse produces an intermediate level population within 10 ns which can, in the absence of additional photons, generate ions in the upper excited state. The delayed maximum in Figure 6c results from the fact that immediately after the laser pulse the upper state population is still essentially zero, but grows in only as
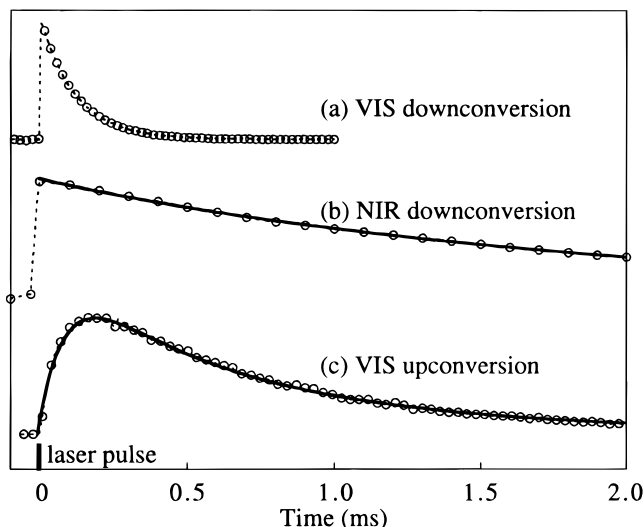
FIGURE 6. 10 K luminescence dynamics observed in 2.5% Re:Cs$_2$-ZrCl$_6$. (a) Visible luminescence with visible excitation, (b) NIR $\Gamma_8(^2T_1) \rightarrow \Gamma_8(^4A_2)$ luminescence with NIR $\Gamma_8(^4A_2) \rightarrow \Gamma_6(^2T_1)$ excitation, and (c) visible $\Gamma_7(^2T_2) \rightarrow \Gamma_8(^4A_2)$ luminescence with a 10-ns NIR $\Gamma_8(^4A_2) \rightarrow \Gamma_6(^2T_1)$ excitation pulse. The solid lines show simulated dynamics calculated from a rate-equation model. Adapted from ref 17.

the intermediate excited ions undergo ETU. Similarly, the long decay in Figure 6c results from the long decay of the intermediate level. The solid lines in Figure 6b,c are transient luminescence curves calculated for the NIR and upconversion luminescence decay transients, respectively, based on a three-level rate equation model using kinetic parameters determined spectroscopically.[17] From the simulation of the variable-temperature time and power dependence data for this system it is possible to determine the branching ratio between luminescence and ETU of the $\Gamma_8(^2T_1)$ excited state. This branching ratio determines the fate of a NIR excited ion and is highly power and concentration dependent, but already favors upconversion over downconversion by a factor of 4 in a moderately

doped (2.5% Re) sample using only 75 mW/mm^2, 1047-nm continuous wave excitation at 300 K. Thus, under readily accessible experimental conditions, *upconversion is the dominant depletion mechanism for the intermediate state*, and not merely a minor side process. The shift from quadratic to linear behavior observed in the power dependence measurements reflects the shift from the low-power regime, in which downconversion is the dominant $\Gamma_8(^2T_1)$ depletion process, to the high-power regime, where upconversion dominates.[17,19]

C. Photon Avalanche in Os^{4+}:Cs$_2$ZrBr$_6$. Os^{4+} has one additional electron relative to Re^{4+}. This introduces significant changes in the excited-state properties, despite the seemingly similar d^3 and d^4 energy-level diagrams of Figures 4a and 7a. In contrast with Re^{4+}, octahedral Os^{4+} has an orbitally degenerate ground state ($^3T_1$). This degeneracy is split by strong spin−orbit coupling (Table 1) into four spinor levels with a total spread of ca. 5000 cm^{-1} (Figure 7b). The 10 K absorption spectrum of 0.2% Os^{4+}:Cs$_2$ZrBr$_6$ is shown in Figure 8a. Several sets of sharp absorption features are observed between 2500 and 17 000 cm^{-1}, due both to excitations involving the ligand-field-independent spin-flip singlet excited states and to transitions within the split ground state (Figure 7). Above 17 000 cm^{-1}, the first Br $\rightarrow$ Os charge-transfer (CT) intensity is observed. The 10 K luminescence spectrum obtained with CT excitation is presented in Figure 8b and shows luminescence originating from the $\Gamma_5(^1T_2)$ (10 315 cm^{-1}) and the higher $\Gamma_1(^1A_1)$ (16 045 cm^{-1}) states.

At low temperatures, visible $\Gamma_1(^1A_1)$ luminescence can also be observed with excitation in the NIR.[16] Three features are observed in the 10 K NIR excitation spectrum of this visible upconversion luminescence (Figure 9a). Remarkably, the most intense upconversion luminescence is observed with excitation energies at which the sample has little or no GSA. The lowest energy feature, at ca. 10 425 cm^{-1}, resembles in energy and shape the $\Gamma_1(^3T_1) \rightarrow \Gamma_3(^1E)/\Gamma_5(^1T_2)$ GSA shown in Figure 9b. To higher energy,
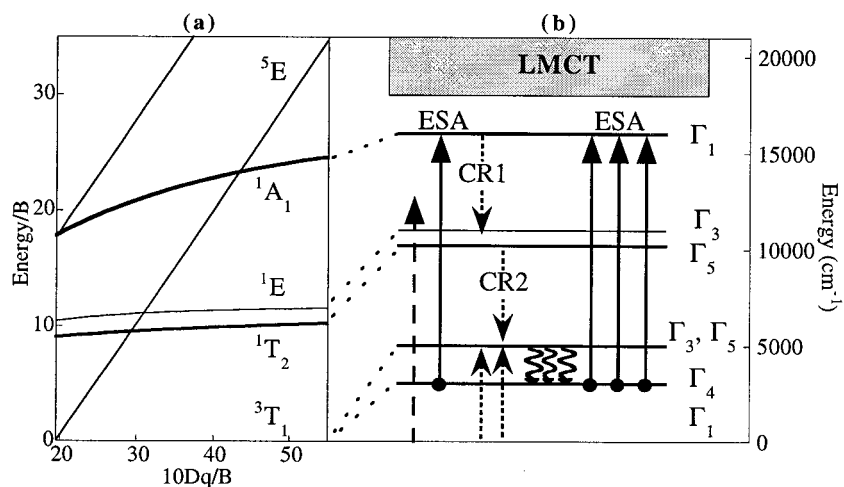

FIGURE 7. (a) Energy-level diagram for a d^4 ion in an octahedral environment, split by spin−orbit interactions in the ground state to yield the levels shown in (b). The luminescent levels in Os^{4+}:Cs$_2$ZrBr$_6$ are shown as bold lines. (b) The photon avalanche mechanism observed with 13 365-cm^{-1} excitation at high pump powers. The long-dash arrow shows the negligible GSA at this excitation energy. The short-dash arrows show the nonradiative energy-transfer cross-relaxation steps, CR1 and CR2, that populate the $\Gamma_4(^3T_1)$ excited state. Curly arrows indicate rapid multiphonon relaxation.
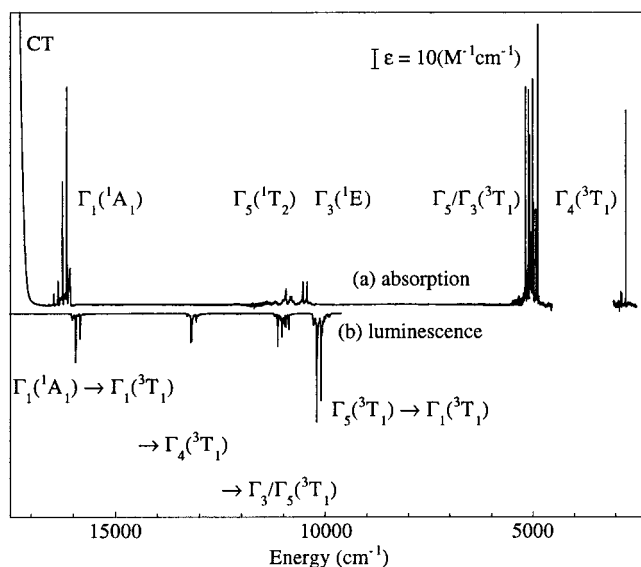
FIGURE 8. 10 K spectra of 0.2% Os^{4+}:Cs_2ZrBr_6 with the transition assignments labeled: (a) absorption and (b) luminescence. Adapted from ref 16.

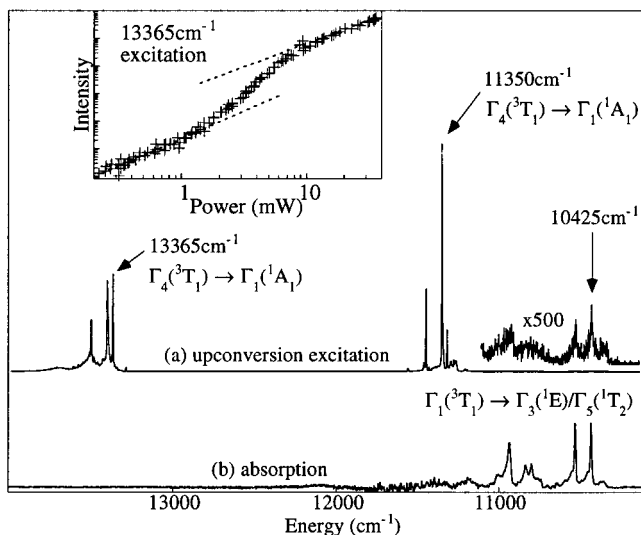**FIGURE 9.** 10 K NIR (a) upconversion excitation and (b) absorption spectra of 0.2% Os^{4+}:Cs_2ZrBr_6. Inset: Logarithmic power dependence of the upconversion luminescence intensity observed with 13 365-cm^{-1} excitation, showing a steep nonlinearity above ca. 1 mW. Adapted from ref 16.

two new features are observed at ca. 11 350 and 13 365 cm^{-1} that have no corresponding features in the GSA spectrum. These features mirror the $\Gamma_1(^1A_1) \rightarrow \Gamma_5(^3T_1)$ and $\Gamma_1(^1A_1) \rightarrow \Gamma_4(^3T_1)$ interexcited-state luminescence transitions and are assigned as the corresponding $\Gamma_5(^3T_1) \rightarrow \Gamma_1(^1A_1)$ and $\Gamma_4(^3T_1) \rightarrow \Gamma_1(^1A_1)$ ESA transitions, respectively. Their dominance clearly indicates the importance of ESA in this system.

Detailed spectroscopic studies have determined that Os^{4+}:Cs_2ZrBr_6 upconversion may proceed by a variety of mechanisms, and that the relative importance of each depends on excitation wavelength and power.[16] The first feature (ca. 10 425 cm^{-1}) in the UC excitation spectrum of Figure 9a has contributions from both GSA/ESA and

GSA/ETU mechanisms. The second feature (ca. 11 350 cm^{-1}) results from a pure GSA/ESA mechanism. The GSA:ESA absorption cross-section ratio at 11 350 cm^{-1} is 1:60 and thus large enough for this excitation sequence. At 13 365 cm^{-1}, corresponding to the third feature in Figure 9a, this GSA:ESA ratio has an upper limit of only 1:600, however, and this changes the excited-state dynamics and the upconversion mechanism dramatically.

Upconversion excited at 13 365 cm^{-1}, corresponding to the $\Gamma_4(^3T_1) \rightarrow \Gamma_1(^1A_1)$ ESA transition, exhibits the very unusual power dependence shown logarithmically in Figure 9 (inset). At low powers, it has a slope of 2. As the power is raised a steep incline is observed above 1 mW, approaching a slope of 4. Above ca. 7 mW the power dependence again levels out to a value of ca. 1.7. There are thus two clearly identifiable regimes in this power dependence: a low-power regime (<1 mW) and a high-power regime (>7 mW). This behavior indicates the presence of two competing mechanisms at this excitation wavelength, a low-power mechanism and a high-power mechanism, with the steep incline reflecting the power region at which the two mechanisms are competitive in efficiency. The data show that in the high-power mechanism the power dependence is reduced and the quantum yield is increased by approximately 2 orders of magnitude relative to those of the low-power mechanism.

The first step in either mechanism must involve excitation by photons at energies where the absorption is essentially zero. Whether through a nonvanishing vibronic or pair GSA cross section at this wavelength, an electronic Raman process, or some other process, ions are promoted to the $\Gamma_4(^3T_1)$ excited state by the laser beam. At 13 365 cm^{-1}, $\Gamma_4(^3T_1) \rightarrow \Gamma_1(^1A_1)$ ESA is efficient, and at low powers this is therefore effectively a GSA/ESA process. This low-power mechanism is relatively inefficient due to the small rate at which the intermediate $\Gamma_4(^3T_1)$ state is populated.

At higher pump powers, a new mechanism takes over in which the relatively inefficient first step is replaced by a more efficient mechanism for populating the intermediate $\Gamma_4(^3T_1)$ state. This mechanism is illustrated in Figure 7b, and begins with an ion excited to $\Gamma_1(^1A_1)$ by the 13 365-cm^{-1} laser. Besides radiative relaxation of the $\Gamma_1(^1A_1)$ state, there is also a very efficient nonradiative cross-relaxation process, designated CR1 in Figure 7b, in which one $\Gamma_1(^1A_1)$-excited ion transfers part of its excitation energy to a ground-state Os^{4+} ion. This is followed by a second cross-relaxation step, CR2 in Figure 7b. As shown in Figure 7b, cross relaxation of one $\Gamma_1(^1A_1)$ excited ion may thus lead to three ions in the $\Gamma_4(^3T_1)$ excited state. At high pump powers, these ions have a significant likelihood of absorbing a photon through ESA, followed again by cross relaxation, and this cycle can be repeated several times until steady-state conditions are reached. The extremely nonlinear buildup of the intermediate excited-state population arising in this way has earned this mechanism the name of photon (or excitation) avalanche. Since the upconversion luminescence intensity is directly related to the population of the intermediate $\Gamma_4(^3T_1)$ state, the avalanche is observed in upconversion luminescence

experiments. An alternative way of monitoring the $\Gamma_4(^3T_1)$ population is by measuring the crystal transmission at the 13 365-cm^{-1} laser energy. It diminishes exactly in the same way as the UC luminescence intensity increases. With the buildup of the avalanche the crystal thus loses its transparency at this wavelength.

In sections IIIA and B we presented examples illustrating two different upconversion mechanisms, GSA/ESA and GSA/ETU. Both examples involved population of an intermediate level by GSA and differed in how ions were subsequently promoted to the upper level. In this section, we have presented an example in which two distinct mechanisms are observed in the same sample and with excitation at the same energy, 13 365 cm^{-1}. Both mechanisms involve ESA as the means of intermediate-to-upper-level excitation, but they differ in how the intermediate level is populated. At low powers (< ca. 1 mW), excitation directly involves the laser beam and may be treated as inefficient GSA. With increasing powers, an iterative ESA/CR1/CR2/ESA... process grows in efficiency and eventually takes over as the principal mechanism for $\Gamma_4(^3T_1)$ population. Upconversion proceeding by the latter mechanism relies on both single-ion ESA transitions and multi-ion energy-transfer steps.

IV. Host Perturbations

The spectroscopic properties of an upconversion material can be modified by placing the active ion into a noninnocent host environment. Here we describe two perturbations that cause dramatic changes in the spectroscopic properties of the Re^{4+} and Ti^{2+} ions discussed above.

A. Host-Sensitized Upconversion. To expand the excitation range available for generating Re^{4+} upconversion, a series of samples have been made involving addition of Yb^{3+} ions as sensitizers into Re^{4+}:Cs$_2$ZrCl$_6$ and Re^{4+}:Cs$_2$NaYCl$_6$.[20] Yb^{3+} provides the material with several intense NIR $^2F_{7/2} \rightarrow {}^2F_{5/2}$ absorption features centered at ca. 10 500 cm^{-1}, easily accessible to Ti^{3+}:sapphire and diode lasers. Excitation into this Yb^{3+} absorption leads to bright red Re^{4+} $\Gamma_7(^2T_2) \rightarrow \Gamma_8(^4A_2)$ luminescence (see Figure 5b). In samples with small Yb^{3+} concentrations, Yb^{3+} luminescence is also observed and has intense features in exact or near resonance with the vibronic $\Gamma_8(^4A_2) \rightarrow \Gamma_6(^2T_1)$ absorption transitions of Re^{4+}. This spectral overlap provides an efficient channel for resonant nonradiative Yb$^{3+} \rightarrow$ Re^{4+} energy transfer. When the RE elpasolite Cs$_2$NaYbCl$_6$ is used as the host with 0.7% Re doping, the Yb$^{3+} \rightarrow$ Re^{4+} energy transfer is essentially quantitative. Yb^{3+} $\rightarrow$ Yb^{3+} energy migration is extremely rapid in this host, and the Re^{4+} dopant ions act as "super traps" for the migrating Yb^{3+} excitation. Re^{4+} ions are efficiently excited in this way and then produce upconversion luminescence via ETU as described in section IIIB. An excitation scheme for this sensitized UC process is shown in Figure 10. Using this sample and Ti^{3+}:sapphire excitation, it has been possible to conveniently generate intense upconversion luminescence at room temperature. While more detailed studies are required to fully understand the dynamics and
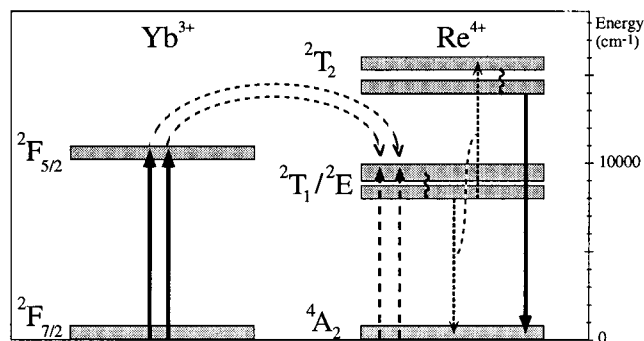

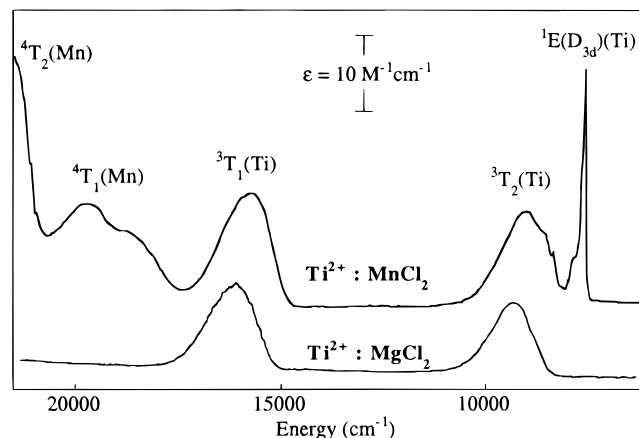**FIGURE 10.** Host-sensitized upconversion mechanism observed in 0.7% Re^{4+}:Cs$_2$NaYbCl$_6$.

FIGURE 11. 10 K axial absorption spectra of Ti^{2+} in the isostructural hosts MnCl$_2$ and MgCl$_2$, showing the effect of a magnetic environment on the intensities of spin-forbidden Ti^{2+} absorption features. Adapted from ref 22.

concentration dependence of this sensitization, the principles of host sensitization and TM/RE combination are well illustrated by this example.

B. Perturbation of Spin Selection Rules by a Magnetic Host. Magnetic interactions can severely influence the spectroscopic properties of a TM.[21] The coupling of magnetic and optical spectroscopic properties has also been targeted as a promising area of supramolecular chemistry in the development of new multifunctional molecular devices. Several of our studies have focused on fundamental properties of magnetic exchange-coupled systems. We are now actively exploring the relationship between spectroscopic, magnetic, and photophysical properties of inorganic materials related to upconversion. Here, we describe results obtained for Ti^{2+}.

As described above, the absorption spin selection rules are rigorously adhered to in both the ground and excited states of Ti^{2+}:MgCl$_2$. In particular, although the $^3T_1$ state lies at twice the energy of the $^1E(D_{3d})$ state, providing a good energetic match for both ESA and ETU, no participation of the spin-forbidden $^1E \rightarrow {}^3T_1$ excitation in Ti^{2+}:MgCl$_2$ upconversion is observed. Figure 11 shows the absorption spectrum of Ti^{2+} substituted into the isostructural host MnCl$_2$.[22] A dramatic increase by more than 2 orders of magnitude in the oscillator strength of the $^3A_2 \rightarrow {}^1E(t_2^2)$ absorption feature is observed. This increased

intensity derives from weak magnetic exchange interactions between the Ti^{2+} ($S = 1$) and its six neighboring paramagnetic Mn^{2+} ions ($S = {}^5/_2$). From a photophysical standpoint, this provides a means of overcoming the stringent spin selection rules of ions such as Ti^{2+}. More generally, it suggests a possibility to regulate the photophysical properties of such species through magnetic interactions. Magnetic exchange interactions are more easily induced in TM systems than in RE systems due to the smaller orbital shielding in TMs, and such effects may therefore be far more pronounced in this relatively unexplored area of TM or mixed TM/RE upconversion. Future studies will address the influence of magnetic perturbations on the excited-state properties of a variety of TM and TM/RE systems, including Ti^{2+},[13] Ni^{2+},[23] and Mo^{3+},[15] all of which have shown the ability to mediate upconversion and also have relatively small spin−orbit coupling parameters (Table 1), leading to stringent selection rules restricting some potentially interesting upconversion processes.

IV. Conclusion

It has been the aim of this Account to summarize a few key results from our research in the area of TM upconversion. A few cases have now been studied in detail, and direct comparison between TM and RE upconversion properties is becoming possible. The examples shown here also suggest two promising avenues for future exploration, namely the combination of TM and RE metals in the same material to exploit their specific excited-state properties, and the tuning of spectroscopic properties through magnetic perturbations using magnetic host materials. The ability of TMs to interact with their environment to a much greater extent than RE ions is in many ways a hindrance because it enhances nonradiative relaxation, which is in competition with upconversion. Alternatively, it provides the opportunity to adjust the photophysical properties of upconversion systems in unprecedented ways through modification of the ligand environment and the magnetic properties of the host. Such modifications have yet to be thoroughly explored, and research in this area will undoubtedly reveal new and unexpected photophysical processes.

References

(1) Blasse, G.; Grabmaier B. C. *Luminescent Materials*; Springer-Verlag: Berlin, 1994.

(2) For example, see: Balzani, V., Ed. *Supramolecular Photochemistry*; D. Reidel Publishing Co.: Dordrecht, The Netherlands, 1987.

(3) For recent examples, see: Riedener, T.; Krämer, K.; Güdel, H. U. Upconversion Luminescence in Er^{3+}-Doped $RbGd_2Cl_7$ and $RbGd_2Br_7$ *Inorg. Chem.* **1995**, *34*, 2745−2752. Hehlen, M. P.; Güdel, H. U.; Shu, Q.; Rand, S. C. Cooperative optical bistability in the dimer system $Cs_3Y_2Br_9$: 10% Yb^{3+}. *J. Chem. Phys.* **1996**, *104*, 1232−1244.

(4) For recent examples, see: Brunold, T. C.; Güdel, H. U.; Riley, M. J. Jahn−Teller effect in the ground and excited states of MnO_4^{2-} doped into Cs_2SO_4. *J. Chem. Phys.* **1996**, *105*, 7931−7941. Hazenkamp, M. F.; Güdel, H. U.; Atanasov, M.; Kesper, U.; Reinen, D. Optical spectroscopy of Cr^{4+}-doped Ca_2GeO_4 and Mg_2SiO_4 *Phys. Rev. B* **1996**, *53*, 2367−2377.

(5) For recent examples, see: Strouse, G. F.; Güdel, H. U.; Bertolasi, V.; Ferretti, V. Optical spectroscopy of single crystal [Re(bpy)(CO)$_4$]-(PF$_6$): Mixing between charge transfer and ligand centered excited states. *Inorg. Chem.* **1995**, *34*, 5578−5587. Vanhelmont, F. W. M.; Rajasekharan, M. V.; Güdel, H. U.; Capelli, S. C.; Hauser, J.; Bürgi, H.-B. Influence of electron donor and acceptor substituents on the excited-state properties of Re(I) tetracarbonyl chelate complexes *J. Chem. Soc., Dalton Trans.* **1998**, 2893−2900.

(6) Wright, J. C. Up-conversion and excited-state energy transfer in rare-earth doped materials. In *Topics in Applied Physics: Radiationless Processes in Molecules and Condensed Phases*; Fong, F. K., Ed.; Springer: Berlin, 1976; pp 239−295.

(7) Lenth, W.; Macfarlane, R. M. Upconversion lasers. *Opt. Photon. News* **1992**, *3*, 8−15. Joubert, M. F. Model of the photon avalanche effect. *Phys. Rev. B* **1993**, *48*, 10031−10037.

(8) McClain, W. M.; Harris, R. A. In *Excited States*; Lim, E. C., Ed.; Academic Press: New York, 1977.

(9) For example, see: Dalton, L. R.; Harper, A. W.; Ghosn, R.; Steier, W. H.; Ziari, M.; Fetterman, H.; Shi, Y.; Mustacich, R. V.; Jen, A. K.-Y.; Shea, K. J. Synthesis and processing of improved organic second-order nonlinear optical materials for applications in photonics. *Chem. Mater.* **1995**, *7*, 1060−1081.

(10) van Dijk, J. M. F.; Schuurmans, M. F. H. On the nonradiative and radiative decay rates and a modified energy gap law for 4f−4f transitions in rare-earth ions. *J. Chem. Phys.* **1983**, *78*, 5317−5323.

(11) Kasha, M. Characterization of electronic transitions in complex molecules *Discuss. Faraday Soc.* **1950**, *9*, 14−19.

(12) Downing, E.; Hesselink, L.; Ralston, J.; Macfarlane, R. A three-color, solid-state, three-dimensional display. *Science* **1996**, *273*, 1185−1189.

(13) Jacobsen, S. M.; Güdel, H. U. Higher excited-state luminescence in Ti^{2+}:$MgCl_2$: Dynamics of radiative and nonradiative processes. *J. Lumin.* **1989**, *43*, 125−137. Jacobsen, S. M.; Güdel, H. U.; Daul, C. A. Excited states of Titanium(2+): Sharp-band and broad-band near-infrared luminescence from Ti^{2+} in $MgCl_2$ and $MgBr_2$. *J. Am. Chem. Soc.* **1988**, *110*, 7610−7616. Jacobsen, S. M.; Herren, M.; Güdel, H. U. Energy transfer in Titanium (II) doped Magnesium Chloride. *J. Lumin.* **1990**, *45*, 369−372.

(14) Wermuth, M.; Güdel, H. U. Upconversion luminescence in a 5d transition-metal ion system: Cs_2ZrCl_6:Os^{4+}. *Chem. Phys. Lett.* **1998**, *281*, 81−85.

(15) Gamelin, D. R.; Güdel, H. U. Two-photon spectroscopy of d^3 transition metals: Near-IR-to-visible upconversion luminescence by Re^{4+} and Mo^{3+}. *J. Am. Chem. Soc.* **1998**, *120*, 12143−12144.

(16) Wermuth, M.; Güdel, H. U. Photon Avalanche in Cs_2ZrBr_6:Os^{4+}. *J. Am. Chem. Soc.* **1999**, *121*, 10102−10111.

(17) Gamelin, D. R.; Güdel, H. U. Spectroscopy and dynamics of Re^{4+} near-IR-to-visible luminescence upconversion. *Inorg. Chem.* **1999**, *38*, 5154−5164.

(18) Lever, A. B. P. *Inorganic Electronic Spectroscopy*, 2nd ed.; Elsevier: Amsterdam, 1984.

(19) Pollnau, M.; Gamelin, D. R.; Lüthi, S. R.; Güdel, H. U.; Hehlen, M. P. Power dependence of upconversion luminescence in lanthanide and transition-metal-ion systems. *Phys. Rev. B* **2000**, *61*, 3337−3346.

(20) Gamelin, D. R.; Güdel, H. U., to be published.

(21) McCarthy, P. J.; Güdel, H. U. Optical spectroscopy of exchange-coupled transition metal complexes. *Coord. Chem. Rev.* **1988**, *88*, 69−131.

(22) Jacobsen, S. M.; Güdel, H. U. Spin cluster excitations in Ti^{2+} doped $MnCl_2$. *J. Lumin.* **1987**, *38*, 184−186.

(23) May, P. S.; Güdel, H. U. One- and two-color sequential two-photon excitation of visible Ni^{2+} luminescence in Ni^{2+}:$CsCdCl_3$. *J. Lumin.* **1990**, *47*, 19−25. Oetliker, U.; Riley, M. J.; May, P. S.; Güdel, H. U. Excited-State Dynamics in Ni^{2+} Doped $CsCdCl_3$: Excitation Avalanche. *Coord. Chem. Rev.* **1991**, *111*, 125−130.

AR990102Y